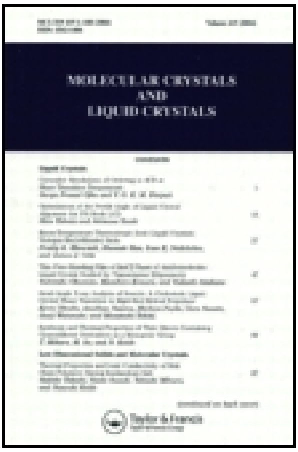

Molecular Crystals and Liquid Crystals
Publication details, including instructions for authors and subscription information:
http://www.tandfonline.com/loi/gmcl20

Synthesis, Characterization, and Anisotropic Properties of 5-Alkoxy-2-((4-(Phenyldiazenyl)Phenylimino)Methyl)phenol and Their Copper(II) Complexes

Guan-Yeow Yeap [a] , Boon-Teck Heng [a] , Makoto Tanabe [b] & Daisuke Takeuchi [b]

[a] Liquid Crystal Research Laboratory, School of Chemical Sciences, Universiti Sains Malaysia, Penang, Malaysia

[b] Chemical Resources Laboratory, Tokyo Institute of Technology, Yokohama, Japan

To cite this article: Guan-Yeow Yeap, Boon-Teck Heng, Makoto Tanabe & Daisuke Takeuchi (2012): Synthesis, Characterization, and Anisotropic Properties of 5-Alkoxy-2-((4-(Phenyldiazenyl)Phenylimino)Methyl)phenol and Their Copper(II) Complexes, Molecular Crystals and Liquid Crystals, 552:1, 217-227

To link to this article: http://dx.doi.org/10.1080/15421406.2011.619097

Mol. Cryst. Liq. Cryst., Vol. 552: pp. 217–227, 2012
Copyright © Taylor & Francis Group, LLC
ISSN: 1542-1406 print/1563-5287 online
DOI: 10.1080/15421406.2011.619097

Synthesis, Characterization, and Anisotropic Properties of 5-Alkoxy-2-((4-(Phenyldiazenyl)Phenylimino)Methyl)phenol and Their Copper(II) Complexes

GUAN-YEOW YEAP,[1,*] BOON-TECK HENG,[1]
MAKOTO TANABE,[2] AND DAISUKE TAKEUCHI[2]

[1]Liquid Crystal Research Laboratory, School of Chemical Sciences, Universiti Sains Malaysia, Penang, Malaysia
[2]Chemical Resources Laboratory, Tokyo Institute of Technology, Yokohama, Japan

A new homologous series of bidentate Schiff bases 5-alkoxy-2-((4-(phenyldiazenyl) phenylimino)methyl)phenol and their Cu(II) complexes have been synthesized and characterized by spectroscopic techniques along with studies on the mesomorphic properties. Phase transitions of all the Schiff bases and Cu(II) complexes in this series are enantiotropic. The ligands with n*-octyloxy and* n*-decyloxy flexible chains exhibit the nematic (N) and smectic A (SmA) phases, the latter of which is characterized by focal conic fan-shaped texture. In contrast, the Cu(II) complexes show exclusively the SmA phase, which is ascribed to the presence of Cu—O and Cu—N coordination modes. For the same reason, the thermal stabilities of the complexes have also been improved.*

Keywords Cu(II) complexes; enantiotropic; nematic; orthogonal smectic A; Schiff bases

1. Introduction

In recent years, a considerable number of metallomesogens have been synthesized and their properties documented [1]. The liquid crystal behaviors of these metal–ligand complexes are claimed to be more prominent than their free ligands owing to the advantages of combining the properties of these ligands with those of transition metals. One of the factors can be attributed to the metal ions that enhance the anisotropic properties of these ligands. As such, the ligands found to be nonmesogenic earlier can change to mesogenic complexes possessing metal–ligand moieties [2].

Metal ions are generally known to possess diverse geometries. As a result, the metallomesogens thus obtained will exist in new geometrical shapes, which may not be observed in the metal-free ligands. These metallomesogens are also much superior to uncoordinated ligands in that the transition metals possess various oxidation states, colors, and magnetisms

---

[*] Address correspondence to Guan-Yeow Yeap, Liquid Crystal Research Laboratory, School of Chemical Sciences, Universiti Sains Malaysia, 11800 Minden, Penang, Malaysia. Fax: 60-4-6574854. E-mail: gyyeap@usm.my; gyyeap_liqcryst_usm@yahoo.com

[3]. It has been reported that the one-dimensional stacking of metal centers could lead to materials with interesting properties such as one-dimensional magnetism and conductivity [4]. Especially, the incorporation of paramagnetic ions in liquid crystalline materials enhances the application of one-dimensional magnet in order to repair the defects in their structure [5] and offers important routes to anisotropic materials that can be readily aligned in the devices [4].

In 1997, Tantrawong and Styring had successfully synthesized the metal containing liquid crystal with the potential application in optical storage [6]. Hayami et al. have reported the mesophase and magnetic behavior in Co(II) and Fe(II) compounds [7]. According to Liu et al., the metallomesogens also possess widespread use as stationary phase in gas chromatographic application [8].

In 2002, Nandiraju et al. reported the influence of metal on the mesomorphic properties of the ligands [9]. A similar study has been carried out by Suste et al. [10].

Besides, the azo-based polymeric liquid crystals and their metal-containing derivatives have also been studied extensively in recent years because these materials are capable of changing the molecular shape through the reversible *cis–trans* isomerization under the influence of UV or photoirradiation. However, it has been claimed that the molecules with −N=N− group prefer the *trans* conformation in mesophase as that reported for photoexcited azo-dye induced torque in N liquid crystals [11].

In spite of these studies, the influence of the metal on the mesophase and correlation between the structure and anisotropic properties of metallomesogens are still subject to further investigation. In this study, a new homologous series of bidentate Schiff bases 5-alkoxy-2-((4-(phenyldiazenyl)phenylimino)methyl)phenol and their Cu(II) complexes have been synthesized to study the influence of the Cu(II) metal ion upon the mesomorphic properties.

2. Experimental

1-Bromooctane, 1-bromodecane, 1-bromododecane, 1-bromotetradecane, and 1-bromohexadecane were purchased from Merck. 4-Aminoazobenzene was purchased from Aldrich Chemical while copper(II) acetate monohydrate and 2,4-dihydroxybenzaldehyde were obtained from Acros Organic. Potassium carbonate was purchased from Systerm.

All the ligands and complexes obtained in this study were characterized by CHN microanalysis, IR spectroscopy, and NMR spectroscopy. CHN microanalyses were carried out using a Perkin Elmer 2400 LS Series CHNS/O analyzer. IR spectra were recorded using a Perkin-Elmer 2000 FT-IR spectrophotometer in the frequency range of 4000–400 cm^{-1}. The IR spectra of all compounds were measured for the samples dispersed in KBr pellets. ^{1}H NMR spectra were recorded on a Bruker 400-MHz Ultrashield FT-NMR spectrometer using $CDCl_3$ as solvent and TMS as the internal standard.

The synthesis of the ligands and corresponding Cu(II) complexes is illustrated in Scheme 1.

2.1. Synthesis of Ligands 1a–1e

Ligands **1a**–**1e** were synthesized by the general procedure as described below.

The mixture containing 4-aminoazobenzene and 2,4-dihydroxybenzaldehyde was heated under reflux in ethanol for 4 h. The precipitate thus formed was isolated and purified with ethanol twice to yield the desired compound. Subsequently, these intermediates were reacted with respective 1-bromooctane, 1-bromodecane, 1-bromododecane,

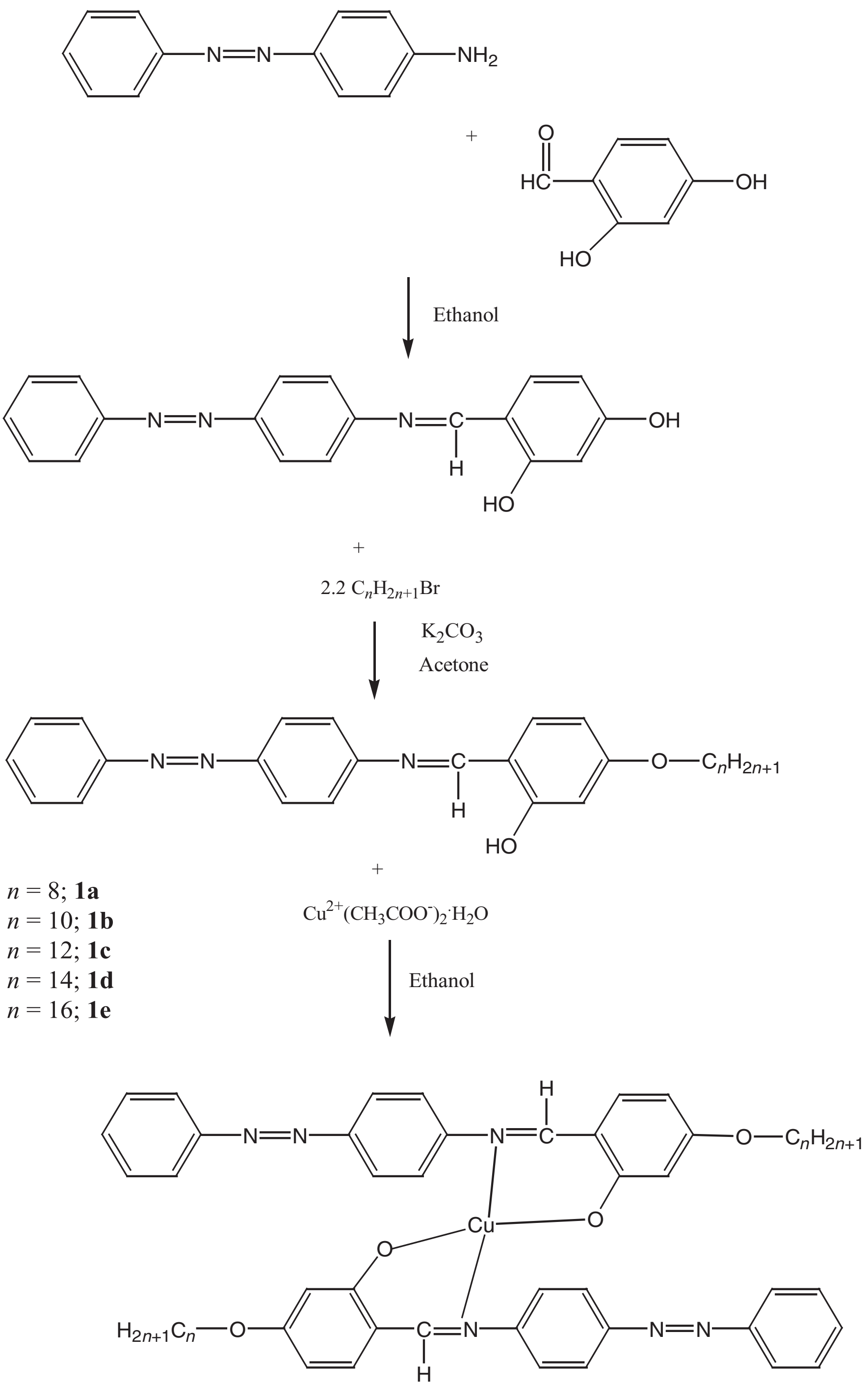

n = 8; **1a**
n = 10; **1b**
n = 12; **1c**
n = 14; **1d**
n = 16; **1e**

n = 8; **2a**
n = 10; **2b**
n = 12; **2c**
n = 14; **2d**
n = 16; **2e**

Scheme 1. Synthetic route to copper(II) complexes.

1-bromotetradecane, and 1-bromohexadecane in the presence of potassium carbonate as base and acetone as the solvent under reflux for overnight. The crude products thus obtained were purified through recrystallization from hexane.

2.2. Synthesis of Copper Complexes 2a–2e

The Cu complexes **2a**–**2e** were prepared using the following method.

Copper(II) acetate monohydrate was dissolved in ethanol and added to a solution of free ligand (**1a**–**1e**) in ethanol. The reaction mixture was stirred and refluxed for 6 h. The brownish crystals were filtered and recrystallized from a solvent mixture of ethanol and chloroform (1:1 v/v).

The analytical data, i.e., IR, 1H NMR spectra data for ligands (**1a**–**1e**) and Cu(II) complexes (**2a**–**2e**), are summarized as follows.

1a: Yield 46%. Elemental analysis/%: found C 75.92, H 7.32, N 9.80; calculated ($C_{27}H_{31}N_3O_2$) C 75.52, H 7.23, N 9.79. IR (KBr)ν_{max}/cm^{-1}: 1625 (C=N), 2848–2954 (C—H alkyl), 1194 (O—CH_2), 1592, 1571 (C=C), 3114–3712 (O—H). ^{1}H NMR (400 MHz, $CDCL_3$) δ/ppm: 0.88–0.91 (t, 3H, CH_3), 1.31–1.87 (m, 12H, CH_2), 4.02–4.05 (t, 2H, CH_2), 6.52–6.55 (m, 2H, Ar), 7.32–7.34 (d, 1H, Ar), 7.41–7.43 (d, 2H, Ar), 7.46–7.57 (m, 3H, Ar), 7.94–7.96 (d, 2H, Ar), 8.00–8.03 (d, 2H, Ar), 8.63 (s, 1H, CH=N), 13.62 (s, 1H, Ar—OH).

1b: Yield 52%. Elemental analysis/%: found C 76.45, H 7.68, N 9.21; calculated ($C_{29}H_{35}N_3O_2$) C 76.15, H 7.66, N 9.19. IR (KBr)ν_{max}/cm^{-1}: 1625 (C=N), 2954–2848 (C—H alkyl), 1194 (O—CH_2), 1592, 1571 (C=C), 3115–3714 (O—H). ^{1}H NMR (400 MHz, $CDCL_3$) δ/ppm: 0.88–0.91 (t, 3H, CH_3), 1.29–1.87 (m, 12H, CH_2), 4.02–4.05 (t, 2H, CH_2), 6.51–6.55 (m, 2H, Ar), 7.31–7.33 (d, 1H, Ar), 7.40–7.43 (d, 2H, Ar), 7.45–7.57 (m, 3H, Ar), 7.93–7.96 (d, 2H, Ar), 8.00–8.03 (d, 2H, Ar), 8.63 (s, 1H, CH=N), 13.60 (s, 1H, Ar—OH).

1c: Yield 50%. Elemental analysis/%: found C 77.01, H 8.14, N 8.70; calculated ($C_{31}H_{39}N_3O_2$), C 76.70, H 8.04, N 8.66. IR (KBr)ν_{max}/cm^{-1}: 1624 (C=N), 2953–2848 (C—H alkyl), 1193 (O—CH_2), 1592, 1571 (C=C), 3115–3714 (O—H). 1H NMR (400 MHz, $CDCL_3$) δ/ppm: 0.88–0.92 (t, 3H, CH_3), 1.25–1.88 (m, 12H, CH_2), 4.02–4.05 (t, 2H, CH_2), 6.51–6.55 (m, 2H, Ar), 7.30–7.33 (d, 1H, Ar), 7.40–7.43 (d, 2H, Ar), 7.46–7.57 (m, 3H, Ar), 7.93–7.96 (d, 2H, Ar), 8.01–8.03 (d, 2H, Ar), 8.63 (s, 1H, CH=N), 13.60 (s, 1H, Ar—OH).

1d: Yield 53%. Elemental analysis/%: found C 77.59, H 8.58, N 8.19; calculated ($C_{33}H_{43}N_3O_2$), C 77.19, H 8.38, N 8.18. IR (KBr)ν_{max}/cm^{-1}: 1625 (C=N), 2953–2849 (C—H alkyl), 1193 (O—CH_2), 1591, 1571 (C=C), 3115–3714 (O—H). ^{1}H NMR (400 MHz, $CDCL_3$) δ/ppm: 0.89–0.93 (t, 3H, CH3), 1.25–1.85 (m, 12H, CH2), 4.02–4.05 (t, 2H, CH2), 6.52–6.54 (m, 2H, Ar), 7.28–7.33 (d, 1H, Ar), 7.40–7.43 (d, 2H, Ar), 7.45–7.57 (m, 3H, Ar), 7.93–7.96 (d, 2H, Ar), 8.01–8.03 (d, 2H, Ar), 8.62 (s, 1H, CH=N), 13.63 (s, 1H, Ar—OH).

1e: Yield 50%. Elemental analysis/%: found C 77.96, H 8.73, N 7.81; calculated ($C_{35}H_{47}N_3O_2$), C 77.63, H 8.69, N 7.76. IR (KBr)ν_{max}/cm^{-1}: 1625 (C=N), 2953–2849 (C—H alkyl), 1192 (O—CH_2), 1591, 1571 (C=C), 3114–3714 (O—H). ^{1}H NMR (400 MHz, $CDCL_3$) δ/ppm: 0.89–0.93 (t, 3H, CH_3), 1.25–1.85 (m, 12H, CH_2), 4.02–4.05 (t, 2H, CH_2), 6.52–6.54 (m, 2H, Ar), 7.28–7.33 (d, 1H, Ar), 7.40–7.43 (d, 2H, Ar), 7.45–7.57 (m, 3H, Ar), 7.93–7.96 (d, 2H, Ar), 8.01–8.03 (d, 2H, Ar), 8.62 (s, 1H, CH=N), 13.63 (s, 1H, Ar—OH).

2a: Yield 80%. Element analysis/%: found C 70.67, H 6.65, N 9.26; calculated ($C_{54}H_{60}N_6O_4Cu$), C 70.46, H 6.53, N 9.14. IR (KBr)ν_{max}/cm^{-1}: 1610 (C=N), 2924–2852 (C—H alkyl), 1206 (O—CH_2).

2b: Yield 75%. Elemental analysis/%: found C 71.66, H 7.03, N 8.73; calculated ($C_{58}H_{68}N_6O_4Cu$), C 71.35, H 6.97, N 8.61. IR (KBr)ν_{max}/cm^{-1}: 1611 (C=N), 2921–2850 (C—H alkyl), 1206 (O—CH_2).

2c: Yield 70%. Elemental analysis/%: found C 72.42, H 7.57, N 8.16; calculated ($C_{62}H_{76}N_6O_4Cu$), C 72.13, H 7.37, N 8.14. IR (KBr)ν_{max}/cm^{-1}: 1611 (C=N), 2921–2851 (C—H alkyl), 1206 (O—CH_2).

2d: Yield 80%. Elemental analysis/%: found C 73.21, H 7.87, N 7.88; calculated ($C_{66}H_{84}N_6O_4Cu$), C 72.82, H 7.72, N 7.72. IR (KBr)ν_{max}/cm^{-1}: 1610 (C=N), 2923–2851 (C—H alkyl), 1206 (O—CH_2).

2e: Yield 80%. Elemental analysis/%: found C 73.87, H 8.17, N 7.46; calculated ($C_{70}H_{92}N_6O_4Cu$), C 73.46, H 8.05, N 7.35. IR (KBr)ν_{max}/cm^{-1}: 1611 (C=N), 2921–2850 (C—H alkyl), 1206 (O—CH_2).

3. Results and Discussion

3.1. Phase Transition and Mesomorphic Properties of Schiff Bases and Related Cu(II) Complexes

Under the polarizing microscope, all the uncoordinated ligands (**1a**–**1e**) and their Cu(II) complexes (**2a**–**2e**) exhibit the phase transitions which are reproducible upon heating and cooling. The transition temperatures and associated enthalpies (kJ mol^{-1}) obtained from differential scanning calorimetry (DSC) are given in Tables 1 and 2, respectively.

When the ligands **1a** and **1b** are cooled down from isotropic liquid, the schlieren texture characteristics of N phase [12] are observed at 173.9°C and 162.6°C, respectively. Further cooling of **1a** and **1b** to respective temperatures of 161.1°C and 159.4°C, has led to the appearance of well-defined focal conic fan-shaped texture characteristics of SmA phase [13]. It is clearly shown in Fig. 1 that the nematic droplets appear and coalesce (Fig. 1(a))

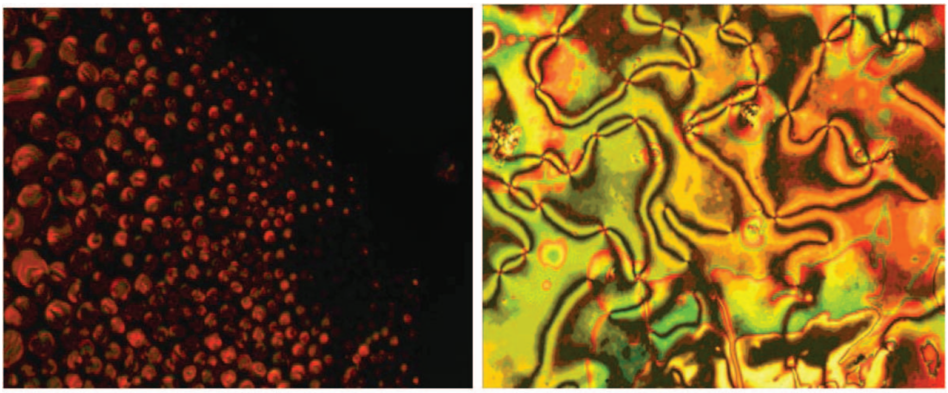
(a) (b)

Figure 1. Photomicrographs of ligand **1a** upon cooling. (a) The small droplets indicate characteristics of the nematic phase; and (b) the schlieren texture of the nematic phase with two-brush and four-brush defects.

Table 1. Phase transition temperature (°C) and associated enthalpies (kJ mol^{-1}) of ligand **1a** ($n = 8$) to **1e** ($n = 16$)

	Heating									Cooling						
Ligand	Cr_1		Cr_2		SmA		N		I	Cr_1	Cr_2	SmA		N		I
1a ($n = 8$)	●	74.2 (5.4)	●	109.7 (30.5)	●	164.3^a	●	176.5^a	●	●	76.1 (−23.5)	●	161.1^a	●	173.9^a	●
1b ($n = 10$)	●	99.6 (7.7)	●	107.1 (27.7)	●	166.9^a	●	168.5 (3.3)	●	●	80.7 (−31.7)	●	159.4^a	●	162.6^a	●
1c ($n = 12$)	●			106.8 (36.3)	●			165.1 (3.2)	●	●	96.1 (−34.0)	●	168.2 (−3.6)			●
1d ($n = 14$)	●			110.3 (64.2)	●			167.9 (6.5)	●	●	91.5 (−66.1)	●	164.6 (−6.0)			●
1e ($n = 16$)	●			112.5 (64.3)	●			164.5 (5.8)	●	●	94.3 (−57)	●	161.7 (−4.7)			●

Cr, crystal; N, nematic; SmA, smectic A; I, isotropic.

[a] Denotes transition temperature derived from unresolved peaks.

Table 2. Phase transition temperature (°C) and associated enthalpies (kJ mol^{-1}) of complexes **2a** ($n = 8$) to **2e** ($n = 16$)

	Heating							Cooling						
Complex	Cr1		Cr2		SmA		I	Cr1		Cr2		SmA		I
2a ($n = 8$)	●			209.4 (45.1)	●	236.7 (7.6)	●	●	171.9 (−40.7)			●	226.9 (−4.9)	●
2b ($n = 10$)	●			207.8 (50.6)	●	239.0 (9.7)	●	●	150.5 (−41.4)			●	227.1[a]	●
2c ($n = 12$)	●			183.8 (39.2)	●	237.5 (10.3)	●	●	149.0 (−29.9)			●	230[a]	●
2d ($n = 14$)	●	125.9 (14.3)	●	179.5 (36.1)	●	233 (10.5)	●	●	123.2 (−10.9)	●	138.9 (−26.1)	●	226.8[a]	●
2e ($n = 16$)	●	130.1 (20.0)	●	171.4 (22.9)	●	225.7 (11.6)	●	●	126.4 (−18.3)	●	141.7 (−23.7)	●	218.4 (−9.4)	●

Cr, crystal; N, nematic; SmA, smectic A; I; isotropic.

[a] Denotes transition temperatures determined via polarizing microscopy, undetected via DSC.

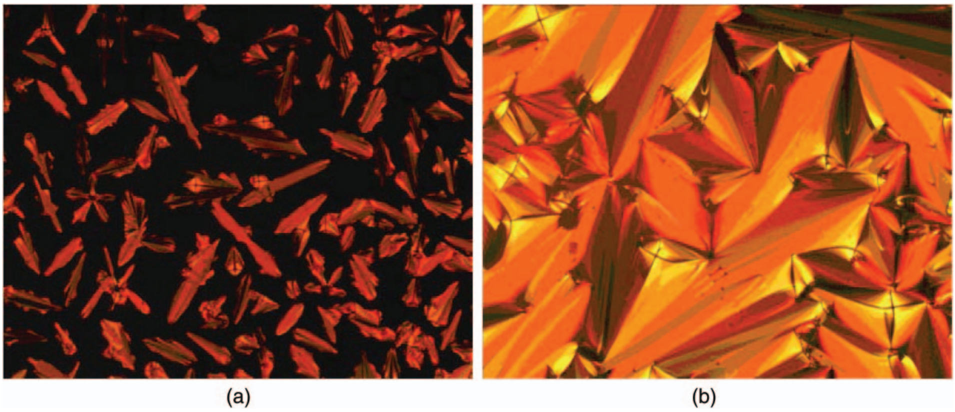

Figure 2. Photomicrographs of ligand **1d** upon cooling. (a) The battonets coalesce to form the focal conic fan-shaped texture of SmA phase as observable in (b).

to form the schlieren texture with two-brush and four-brush defects (Fig. 1(b)) [14]. From Table 1, the mesomorphic range for N phase decreases when the number of carbon atoms in the flexible alkoxy chain increases from $n = 8$ to $n = 10$.

The N phase is not observed upon further lengthening of the alkoxy chain in the ligand ranging from **1c** ($n = 12$) to ligand **1e** ($n = 16$). Instead, these ligands exhibit only enantiotropic SmA phase. The presence of SmA phase can be evident by the formation of battonets that coalesce to form the fan-shaped texture (Fig. 2) [15]. This shows that with the increase in the length of the flexible terminal chain, the nematogenic properties decrease leading to the formation of the SmA phase. This phenomenon can be explained by the hydrophobic interaction between the long flexible terminal chains leading to their intertwining, which facilitates the lamellar packing and is essential for the smectic phase [16].

The smectogenic properties of the ligands can also be ascribed to the presence of a hydroxyl group in the *ortho* position, which enhances the transverse dipole moment and intramolecular as well as intermolecular interactions. As such, it helps to stabilize the molecule and promotes ordered mesophase [9].

Correlation of phase transition temperatures and the carbon number of the flexible chain in uncoordinated ligands is illustrated in Fig. 3. In this figure, it is shown that the clearing points of the ligands are almost independent of the length of the flexible alkoxy chain in which the carbon numbers are even.

All the Cu(II) complexes (**2a**–**2e**) show enantiotropic SmA phase with focal conic fan-shaped texture as shown in Fig. 2. The lower homologues of complexes with $n = 8$ and $n = 10$ exhibit only SmA phase in comparison to the uncoordinated ligands with the same n exhibiting both N and SmA phases. The suppression of N phase can be caused by the greater polarity of the coordination bonds in CuL_2 that enhances transverse intermolecular association, promoting the formation of SmA phase [3]. This can also result from the differences of molecular geometry between the ligand and the Cu(II) complex [3]. Although the Cu(II) complexes with $n = 12$, 14, and 16 retain the same mesophases as those appear in the free ligands, the mesomorphic range shifts to the higher temperature side upon complexation.

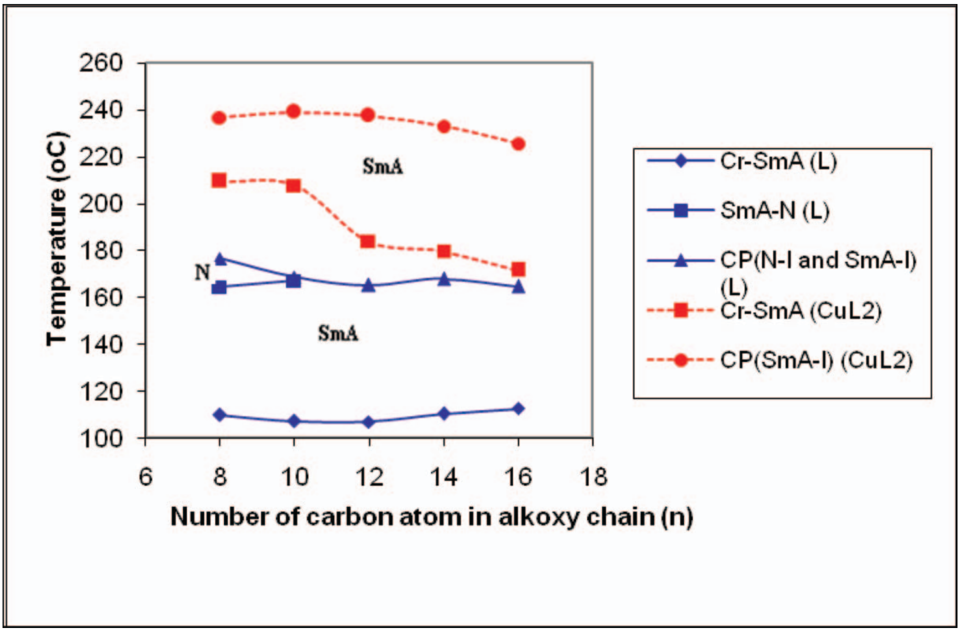

Figure 3. A plot of phase transition temperature upon heating versus the number of carbon atoms in the alkoxy chain for the ligands **1a–1e**, L (solid line), and their copper(II) complexes, CuL2 (dotted line) (Color figure available online).

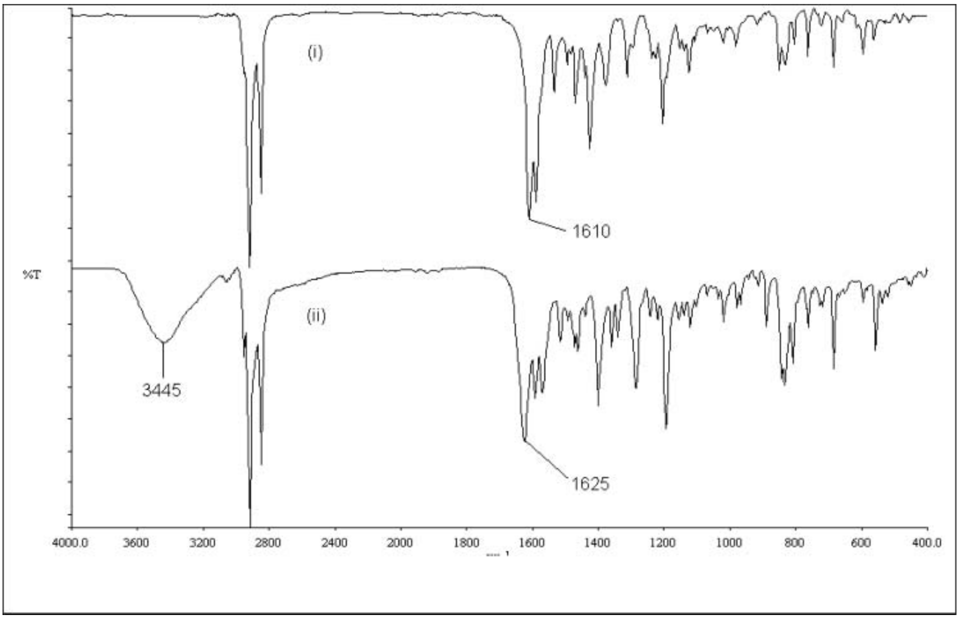

Figure 4. Representative IR spectra of (i) Cu(II) complex **2e**; and (ii) ligand **1e**, shifted vertically.

From Tables 1 and 2, and Fig. 3, a general trend can be noted. The transition temperatures for all the Cu(II) complexes are significantly higher than those of the free ligands and decrease as the number of carbon atoms in flexible alkoxy chain increases. Besides, the clearing temperatures of Cu(II) complexes increase by 60°C–70°C upon complexation. The enthalpy change associated with the clearing point for the Cu(II) complex, which is higher than that for the corresponding free ligand, increases with the increase in the molecular length.

3.2. Spectroscopic Studies

Upon complexation with Cu(II) acetate, the signals attributed to all the protons in close proximity with the paramagnetic Cu(II) centers are not observed and their ^{1}H NMR spectra display only a broad signal indicating the presence of alkoxy group [1]. These results confirm the coordination of the ligand to the central Cu(II) atom. The representative IR spectra are shown in Fig. 4. All the IR spectra of metal complexes show the stretching mode of the C=N bond in the range of 1610–1611 cm^{-1}, which is shifted to lower frequency than the free ligand (1624–1625 cm^{-1}) [1, 3, 5, 9, 11]. This observation can be ascribed to the reduction of double bond character of the C=N bond and this supports the coordination of the ligand N atom to the central Cu(II) atom. On the other hand, the stretching frequency of the phenolic OH group in the Cu(II) complexes is absent. This indicates that the OH group is in the deprotonated state as a result of the coordination of this ligand to the Cu(II) center through negatively charged O.

4. Conclusions

A new homologous series of bidentate Schiff base 5-alkoxy-((4-(phenyldiazenyl)phenylimino)methyl)phenol and their Cu(II) complexes with flexible terminal alkoxy chain in even parity ranging from $n = 8$ to $n = 16$ have been synthesized and characterized. The phase transitions of all ligands and their Cu(II) complexes are enantiotropic. The ligands with *n*-octyloxy and *n*-decyloxy flexible chains are found to exhibit N and the SmA phase (the latter of which is suggested by focal conic fan-shaped texture), while all the Cu(II) complexes exhibit the SmA phase. The transition temperatures and clearing points for all the Cu(II) complexes are significantly higher than those of the free ligands.

Acknowledgments

The main author (G.-Y. Yeap) would like to thank Universiti Sains Malaysia for the FRGS Grant No. 203/PKIMIA/6711192 and Incentive Grant No. 1001/PKIMIA/822208.

References

[1] Rezvani, Z., Divband, B., Abbasi, A. R., & Nejati, K. (2006). *Polyhedron*, *25*, 1915–1920.
[2] Lee, C. K., Ling, M. C., & Ivan Lim, J. B. (2003). *J. Chem. Soc. Dalton Trans.*, 4731–4737.
[3] Suste, A., & Sunjic, V. (1996). *Liq. Cryst.*, *20*, 219–224.
[4] Trzaska, S. T., & Swager, T. M. (1998). *Chem. Mater.*, *10*, 438–443.
[5] Pucci, D., Aiello, I., Bellusci, A., Callipari, G., Crispini, A., & Ghedini, M. (2009). *Mol. Cryst. Liq. Cryst.*, *500*, 144–154.
[6] Tantrawong, S., & Styring, P. (1997). *Liq. Cryst.*, *22*, 17–22.
[7] Hayami, S., Kojima, Y., Urakami, D., Ohta, K., & Inoue, K. (2009). *Polyhedron*, *28*, 2053–2057.

[8] Liu, C. Y., Chen, J. L., Shiue, C. C., & Liu, K. T. (1999). *J. Chromatogr. A.*, *862*, 65–83.

[9] Nandiraju, V. S., Singha, D., Das, M., & Paul, M. K. (2002). *Mol. Cryst. Liq. Cryst.*, *373*, 105–117.

[10] Suste, A., & Sunjic, V. (1996). *Liq. Cryst.*, *20*, 219–224.

[11] Saad, A., Galstyan, T. V., Denariez-Roberge, M. M., & Dumont, M. (1998). *Opt. Commun.*, *151*, 235–240.

[12] Ha, S. T., Ong, L. K., Wong, P. W., Yeap, G.-Y., Lin, H. C., Ong, S. T., & Koh, T. M. (2009). *Phase Transitions*, *5*, 387–397.

[13] Ha, S. T., Ong, L. K., Lee, S. L., Lin, H. C., Win, Y. F., & Ong, S. T. (2010). *Chin. Chem. Lett.*, *21*, 637–640.

[14] Ha, S. T., Koh, T. M., Yeap, G.-Y., Lin, H. C., Beh, J. K., Win, F. Y., & Boey, P. L. (2009). *Chin. Chem. Lett.*, *20*, 1081–1084.

[15] Ha, S. T., Ong, L. K., Ong, S. T., Yeap, G.-Y., Wong, P. W., Koh, T. M., & Lin, H. C. (2009). *Chin. Chem. Lett.*, *20*, 767–770.

[16] Gray, G. W. (1962). *Molecular Structure and Properties of Liquid Crystals*, Academic Press: London.